Weak seed banks influence the signature and detectability of selective sweeps

Kevin Korfmann[1*], Diala Abu Awad,[1,2], Aurélien Tellier[1]

[1] Professorship for Population Genetics, Department of Life Science Systems, School of Life Sciences, Technical University of Munich, Germany

[2] Université Paris-Saclay, INRAE Le Moulon, France

[*] Corresponding author, kevin.korfmann@tum.de

Abstract

Seed banking (or dormancy) is a widespread bet-hedging strategy, generating a form of population overlap, which decreases the magnitude of genetic drift. The methodological complexity of integrating this trait ~~means~~ implies it is ignored when developing tools to detect selective sweeps. But, as dormancy lengthens the ancestral recombination graph (ARG), increasing times to fixation, it can ~~radically~~ change the genomic signals of selection. To detect genes under positive selection in seed banking species it is important to 1) determine whether the efficacy of selection is affected, and 2) predict the patterns of nucleotide diversity at and around positively selected alleles. We present the first tree sequence-based simulation program integrating a weak seed bank to examine the dynamics and genomic footprints of beneficial alleles in a finite population. We find that seed banking ~~generally decreases~~ does not affect the probability of fixation and ~~magnifies (respectively decreases) the efficacy of selection for alleles under strong (respectively weak) selection~~confirm expectations of increased times to fixation. We also confirm earlier findings that, for strong selection, the times to fixation are not scaled by the inbreeding effective population size in the presence of seed banks, but are shorter than would be expected. As seed banking increases the effective recombination rate, footprints of sweeps appear more narrow around the selected sites and due to the scaling of the ARG are detectable for longer periods of time. The developed simulation tool can be used to predict the footprints of selection and draw statistical inference of past evolutionary events in plants, invertebrates, or fungi with seed banks.

Keywords— seed bank, weak, dormancy, selection, tskit, tree sequence, forward simulation, fixation time, fixation probability, ancestral recombination graph

1 Introduction

Seed banking is an ecological bet-hedging strategy, by which seeds or eggs lay in a dormant state of reduced metabolism until conditions are more favourable to hatch or germinate and complete the life-cycle. This life-history trait acts therefore as a buffer in uncertain environments (~~Cohen 1966; Templeton and Levin 1979~~ Cohen, 1966; Templeton and Levin, 1979) and has evolved several times independently in prokaryotes, fungi, plants, and invertebrates (~~Evans and Dennehy 2005; Willis et al. 2014; Tellier 2019; Lennon et al. 2021~~ Evans and Dennehy, 2005; Nara, 2009; Willis et al., 2014; Tellier, 2019; Lennon et al., 2021). Because several generations of seeds are simultaneously maintained, seed banks act as a temporal storage of genetic information (~~Evans and Dennehy 2005~~Evans and Dennehy, 2005), decreasing the effect of genetic drift and lengthening the time to fixation of neutral and selected alleles (~~Templeton and Levin 1979; Hairston Jr an~~ Templeton and Levin, 1979; Hairston Jr and De Stasio Jr, 1988). Seed banks ~~play therefore~~ are therefore expected to play an important role ~~as the maintenance of genetic diversity is central to~~ in determining the adaptive potential of a species (Tellier, 2019). In bacteria (~~Shoemaker and Lennon 2018; Lennon et al. 2021~~ Shoemaker and Lennon, 2018; Lennon et al., 2021), invertebrates (~~Evans and Dennehy 2005~~Evans and Dennehy, 2005) or plants (~~Willis et al. 2014; Tellier 2019~~Willis et al., 2014; Tellier, 2019), dormancy determines the neutral and selective diversity of populations ~~/species~~ by affecting the effective population size and buffering population size changes (~~Nunney and Ritland 2002), mutation rate (Levin 1990; Whittle 2006; Dann et al. 2~~ Nunney and Ritland, 2002), affecting mutation rates (Levin, 1990; Whittle, 2006; Dann et al., 2017), spatial structure (~~Vitalis et al. 2004~~Vitalis et al., 2004), rates of population extinction/recolonization (~~Brown and Kodric-Brown 1977; Manna et al. 2017~~Brown and Kodric-Brown, 1977; Manna et al., 2017) and the efficacy of positive (~~Hairston Jr and De Stasio Jr 1988; Koopmann et al. 2017; Heinrich et al. 2018; Shoemaker~~ Hairston Jr and De Stasio Jr, 1988; Koopmann et al., 2017; Heinrich et al., 2018; Shoemaker and Lennon, 2018) and balancing selection (~~Tellier and Brown 2009; Verin and Tellier 2018~~Tellier and Brown, 2009; Verin and Tellier, 201).

Seed banking, or dormancy, introduces a time delay between the changes in the active population (above-ground for plants) and changes in the dormant compartment (seeds for plants) which considerably increases the time to reach the common ancestor of a ~~sample or population (Kaj et al. 2001; Blath et al. 2015, 2016, 2020~~population (Kaj et al., 2001; Blath et al., 2015, 2016, 2020). We note that two models of seed banks are proposed, namely the weak and strong dormancy models. These make different assumptions regarding the scale of the importance of dormancy relative to the evolutionary history of the species. On the one hand, the strong version is conceptualized after a modified two-island model with coalescent events occurring only in the active compartment as opposed to the dormant compartment (seed bank) with migration (dormancy and resuscitation) between the two (~~Blath et al. 2015, 2016, 2019; Shoemaker and Lennon 2018~~Blath et al., 2015, 2016, 2019; Shoemaker and). Strong seed bank applies more specifically to organisms, such as bacteria or viruses, which exhibit very quick multiplication cycles and can stay dormant for times on the order of the population size (thousands to millions of generations, ~~Blath et al. 2015, 2020; Lennon et al. 2021~~Blath et al., 2015, 2020; Lennon et al., 2). On the other hand, the weak seed bank model assumes that dormancy occurs only over a few (tens to ~~hundred) generations~~hundreds) generations, thus seemingly negligible when compared to the

population size order of magnitude of the population size (Kaj et al., 2001; Tellier et al., 2011; Živković and Tellier, 2012;), making it applicable to plant, fungi or invertebrate (*e.g. Daphnia sp.*) species (Kaj et al. 2001; Tellier et al. 2011; Živko or when the seed banks is experimentally imposed (as it is in practice difficult to generate the strong seed bank) (Shoemaker et al., 2022). We focus here on the weak seed bank model as we in order to provide novel insights into the population genomic analysis of plant, fungi and invertebrate species which undergo sexual reproduction. We come back in the discussion on the The applicability of our resultsby highlighting , as well as the differences and similarities between the strong and weak seed bank models, are highlighted in the Discussion.

The weak seed bank model can be formulated forward-in-time as an extension of the classic Wright-Fisher model for a population of size N haploid individuals. The constraint of choosing the parents of offspring at generation t only from the previous generation $(t-1)$ is lifted, and replaced with the option of choosing parents from previous generations $(t-2, t-3, ...$ up to a predetermined boundary $t-m)$(Nunney and Ritland 2002Nunney and Ritland, 2002). The equivalent backward-in-time model extends the classic Kingman coalescent and assumes an urn model in which lineages are thrown back-in-time into a sliding window of size m generations, representing the populations of size N from the past (Kaj et al. 2001Kaj et al., 2001). Coalescent events occur when two lineages choose randomly randomly choose the same parent in the past. The germination probability of a seed of age i is b_i, which is equivalent to the probability for one offspring to choose of one offspring choosing a parent i generations ago. The weak dormancy model is shown to converge to a standard Kingman coalescent with a scaled coalescent rate of $1/\beta^2$, in which $\beta = \frac{\sum_{i=1}^{m} b_i}{\sum_{i=1}^{m} i b_i}$ is the inverse of the mean time seeds spend in the seed bank, and m is the maximum time seeds can be dormant (Kaj et al. 2001Kaj et al., 2001). The intuition in a coalescent framework (Kaj et al., 2001) is that for two lineages to find a common ancestor, *i.e.* to coalesce, they need to choose the same parent in the above-ground population, and have each the probability β to do so as only active lineages can coalesce. Thus the probability that two lineages are simultaneously in the active population is β scaling the coalescent rate. The germination function was previously simplified by assuming that the distribution of the germination rate follows a truncated geometric function with rate b, so that $b = \beta$ when m is large enough (Tellier et al. 2011; Živković and Tellier 2012; Sellinger et al. 2019 Tellier et al., 2011; Živković and Tellier, 2012; Sellinger et al., 2019, see methods). A geometric germination function is also assumed in the forward-in-time diffusion model analysed in Koopmann et al. 2017; Heinrich et al Koopmann et al., 2017; Heinrich et al., 2018; Blath et al., 2020.

Seed banking influences therefore neutral and selective processes via its influence on the rate of genetic drift. In a nutshell, a seed bank delays the time to fixation of a neutral allele and increase the increases the inbreeding effective population size (from now on referred to only by effective population size) by a factor $1/b^2$. The effective population size under a weak seed bank is defined as $N_e = \frac{N_{cs}}{b^2}$ where N_{cs} is the census size of the above-ground population (Nunney and Ritland 2002; Tellier et al. 2011; Živković and T Nunney and Ritland, 2002; Tellier et al., 2011; Živković and Tellier, 2012). Mutation under an infinite site model can occur in seeds with probability μ_s and μ_a in the active population (above-ground for plants), so that we can define θ the population mutation rate under the weak seed bank model:

$\theta = \frac{4N_{cs}(b\mu_a+(1-b)\mu_s)}{b^2}$ (~~Tellier et al. 2011~~Tellier et al., 2011). If mutations occur in seeds at the same rate as above-ground (in pollen and ovules), we define $\mu_s = \mu_a = \mu$ yielding ~~$\theta = \frac{4N_{cs}\mu)}{b^2}$~~ $\theta = \frac{4N_{cs}\mu}{b^2}$, while if seeds do not mutate, $\mu_s = 0$ and $\mu_a = \mu$, yielding $\theta = \frac{4N_{cs}\mu}{b}$. Empirical evidence (~~Levin 1990; Whittle 2006; Dann et al. 2017~~Levin, 1990; Whittle, 2006; Dann et al., 2017) and molecular biology experiments showing that even under reduced metabolism DNA integrity has to be protected (~~Waterworth et al. 2016~~Waterworth et al., 2016), suggest that mutations occur in seeds (for simplicity at the same rate as above-ground~~for simplicity) as assumed in most weak seed bank models~~, see model in Sellinger et al., 2019). Furthermore, recombination and the rate of crossing-over is also affected by seed banking. ~~Only one lineage is , however,~~ However, only the non-dormant lineage is affected by recombination in the backward-in-time model so that the population recombination rate is $\rho = 4N_e rb = \frac{4N_{cs}r}{b}$. ~~Indeed, the~~ The recombination rate r needs to be multiplied by the probability of germination b as only active individuals can recombine (~~Živković and Tellier 2018; Sellinger et al. 2019). Importantly, the~~ Živković and Tellier, 2018; Sellinger et al., 2019). The balance of population mutation rate and recombination rate defines the amount of nucleotide diversity in the genome as well as the amount of linkage disequilibrium, a property which ~~we~~ has been used to develop an Sequential Markovian Coalescent (SMC) approach to jointly estimate past demographic history and the germination rate (~~Sellinger et al. 2019, 2021~~Sellinger et al., 2019, 2021).

While there is now a thorough understanding of how neutral diversity is affected by seed banking, the dynamics of alleles under selection have not been fully explored. ~~Koopmann et al. 2017~~ Koopmann et al., 2017 developed a diffusion model of infinite (deterministic) seed bank model with positive selection and show ~~surprisingly~~ that the time to fixation is not multiplied by $1/b^2$ (as for neutral alleles) but at a smaller rate. The interpretation is as follows: while the time to fixation of an advantageous allele is lengthened compared to a model without dormancy, the efficacy of selection should be ~~increased~~ altered compared to a neutral allele (the effect of genetic drift). Namely, the Site Frequency Spectrum (SFS) of independently selected alleles shows an increased deviation from neutrality with a decreasing value of b. ~~This result is confirmed in Heinrich et al. 2018 in which~~ By relaxing the deterministic seed bank assumption~~is relaxed, generating two additional insights~~, Heinrich et al., 2018 find that: 1) a finite small seed bank decreases the efficacy of selection, and 2) selection on fecundity (production of offspring/seeds) yields different selection efficiency ~~from the~~ compared to selection on viability (seed viability)~~as observable in the~~ , as can be seen from their estimated Site-Frequency Spectrum (SFS) of independent alleles under selection. Furthermore, based on the effect of seed bank θ and ρ and on selection, verbal predictions on the genomic signatures of selection have been put forth (~~Živković and Tellier 2018~~Živković and Tellier, 2018).

These theoretical and conceptual ~~studies~~approaches, while paving the way for studying selection under seed banks, did not consider the following argument. If the time to fixation of an advantageous ~~alleles~~ allele increases due to the seed bank, it can be expected that 1) drift has more time to drive this allele to extinction, and 2) the signatures of selective sweeps can be erased by new mutations appearing in the vicinity of the selected alleles. These effects would counter-act ~~the predictions~~

from 1) Koopmann et al. 2017 Koopmann et al.'s (2017) predictions that selection is more efficient under a stronger seed bank compared to genetic drift, and 2) from Živković and Tellier 2018 as well as Živković and Tellier's (2018), that selective sweeps are more easily observable under stronger seed bank. It is the aim of the present study In order to resolve this paradox. We therefore , we develop and make available the first simulation method for the weak seed bank modelwhich allows generating , which allows users to generate full genome data under neutrality and selection. We first present a simulation modelin which we the simulation model, which we use to follow the frequencies of an adaptive allele in a population with seed banking, and examine the ensuing selective sweeps to predict times to, probabilities and detection of allele fixation. Therefore, this study aimed . We aim to provide insights into the characteristics of selective sweeps, including the time and probability of fixation, as well as suggestions recommendations for their detection in species exhibiting seed banks.

2 Methods

Forward-in-time individual-based simulations are implemented in C++. Genealogies are stored and manipulated with the tree sequence toolkit (tskit, Kelleher et al. 2018Kelleher et al., 2018), which allows for a general approach to handling arbitrary evolutionary models and an efficient workflow through well-documented functions.

2.1 Model

The model represents a single, panmictic population of N hermaphroditic diploid adults. Population size is fixed to $2N$ and generations are discrete. In the absence of dormancy and selection, the population follows a classic Wright-Fisher model. In this case, at the beginning of each generation, new individuals are produced by sampling parents from the previous generation. Parents are sampled with probability $\frac{1}{N}$ (multinomial sampling), leading to two vectors $\mathbf{X}_{parent1}$ and $\mathbf{X}_{parent2}$, containing the indicies of the respective parents:

$$X_{parent} \sim Mult(N, \tfrac{1}{N}) \; \mathbf{X}_{parent1} = (X_1^1, X_2^1, ..., X_N^1) \sim Mult(N, \tfrac{1}{N}) \text{ with } \{X_i^1 \in \mathbb{N} : X_i^1 \leq N\}$$

$$\mathbf{X}_{parent2} = (X_1^2, X_2^2, ..., X_N^2) \sim Mult(N, \tfrac{1}{N}) \text{ with } \{X_i^2 \in \mathbb{N} : X_i^2 \leq N\}$$

Once sampled, each parent contributes a (recombined) gamete to generate the new individual. Dormancy adds a layer of complexity, by introducing seeds that can germinate after being dormant for many generations. This relaxes the implicit Wright-Fisher assumption, as parents are no longer only sampled from the previous generation, but also from seeds produced up to m generations agoin the past. The probability of being sampled from generation k_i k depends on the probability of germination, which is a function of the age of the dormant seed. Parents are sampled using a probability vector Y_i^{norm} $\mathbf{Y}^{norm}$ written as:

$$\Pr(Y_i = k_i) = (1-b)^{k_i - 1} b$$

from which we obtain:

$$Y_i^{norm} = \frac{Y_i}{\sum_{j=1}^{m} Y_j}$$

$$\mathbf{Y} = (Y_1, Y_2, Y_k, ..., Y_m) \text{ with } \Pr(Y_k) = b(1-b)^{k-1} \text{ and } \{Y_k \in \mathbb{R} : Y_k > 0\}$$

$$\text{from which we obtain: } \mathbf{Y}_k^{norm} = \frac{Y_k}{\sum_{j=1}^{m} Y_j}$$

From the expression above, the probability of being sampled follows a truncated geometric distribution parameterized with germination rate b and then normalized. The generation G of each parent is randomly sampled using a multinomial sampling with the probability vector ~~Y_i^{norm}~~Y^{norm}.

$$G_{parent1} \sim Mult(m, Y_i^{norm})$$

$$\mathbf{G}_{parent1} = (G_1^1, G_2^1, ..., G_N^1) \sim Mult(N, \mathbf{Y}^{norm}) \text{ with } \{G_i^1 \in \mathbb{N} : G_i^1 \leq N\}$$

$$\mathbf{G}_{parent2} = (G_1^2, G_2^2, ..., G_N^2) \sim Mult(N, \mathbf{Y}^{norm}) \text{ with } \{G_i^2 \in \mathbb{N} : G_i^2 \leq N\}$$

Once the age of each of the parents has been determined, a random individual from each of the sampled age groups is picked, and a gamete ~~is generated~~ (representing a long chromosome sequence), which contributes to creating an offspring, is generated. Gametes are produced by recombination using the two initial genome copies carried by the sampled parent. The number of recombination events is sampled from a Poisson distribution with parameter r (for example 1×10^{-8} per bp per generation). At the end of this process, new mutations can be introduced ~~. Unless stated otherwise, mutations are neutral and the number of new mutations is sampled analogously from a Poisson distribution with rate parameter μ~~(only necessary for sweep detection tools). Generally neutral mutations are not simulated and statistics are computed using branch lengths. We assume here that mutations are also introduced at every generation in dormant individuals at the same rate (~~see justification in Sellinger et al. 2019~~)following Sellinger et al., 2019), even if they are not explicitly simulated. Recombination breakpoints ~~and mutations are distributed uniformly~~ are uniformly distributed across the genome with each coalescent tree being delineated by two recombination breakpoints. In other words, we use the Sequantially Markovian Coalescent approximation of the Ancestral Recombination Graph, McVean and Cardin, 2005).

To model selection signatures within a neutral genomic background, we consider non-neutral bi-allelic loci, placed at predefined and fixed genomic positions, with beneficial mutations arising after the burn-in period. ~~The~~ A locus under selection has a dominance h and selection coefficient s, respectively. The expressions for the fitness of heterozygote and homozygote individuals are thus $1 + hs$ and $1 + s$, respectively. Fitness affects the probability that an individual germinates and becomes a reproducing adult. In the case of dormancy, the choice of the germinating generation when sampling the parents is unaffected by their fitness values, but the sampling of individuals within a given generation is determined by the fitness. In other words, selection acts on fecundity,

as the fitness of an allele determines the number of offspring produced and not the survival of the seed (viability selection). A selection coefficient of 0 would lead to multinomial Wright-Fisher sampling, which can be used to track neutral mutations over time. This two-step process of first choosing the generation ~~and afterwards~~ followed by the individual is presented in Figure 1. ~~In other words, selection acts on fecundity as the fitness of an allele determines the number of offspring produced and not the survival of the seed (viability selection).~~

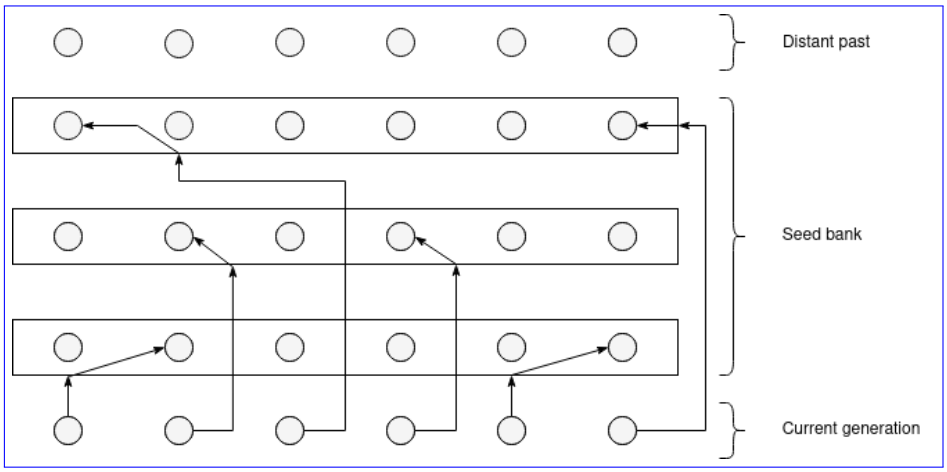

Fig. 1. Schematic representation of the weak dormancy seed bank model by a forward-in-time two step process (~~Kaj et al. 2001~~Kaj et al., 2001). The arrows originating from the current generation represent the geometric sampling process of the parent or seed generation, while the second arrow constitute the sampling of the individual within the given generation based on the respective fitness value.

From a technical perspective, individuals ~~are stored~~ can be tracked in the tskit-provided table data structures, if the *tree_sequence_recording* feature is enabled. This feature is not required when computing statistics on allele frequency dynamics only (*i.e.* to compute fixation times or probabilities). The tables used in this simulation are as follows: 1) a node table representing a set of genomes, 2) an edge-table defining parent-offspring relationships between node pairs over a genomic interval, 3) a site table to store the ancestral states of positions in the genome, and 4) a mutation table defining state changes at particular sites. The last two tables are only used to add the selective mutation. Neutral mutations are simulated afterward, if required for down-stream analysis. The simulation code works with these tables through tskit functions, e.g. the addition of information to a table after sampling a particular individual or through the removal of parents who do not have offspring in the current generation in a recurrent simplification process. This clean-up process is a requirement to reduce RAM-usage during the simulation, because keeping track of every individual ever simulated for building the genealogy afterward, quickly becomes infeasible. However, a noticeable difference to the classic use of the tskit function is in our case that individuals which have not produced offspring in the past, but are still within the dormancy upper-bound defined range of m generations, need to be ~~kept as well during~~ protected from the simplification process, which is achieved by marking them as *sample nodes* during the simulation. Indeed, forward-in-time, a par-

ent can give offspring many generations later (maximum m) through germinating seeds. ~~Selective mutations are tracked externally in order to avoid the time-consuming step of generating a genotype matrix from tskittables at every generation to determine fitness values per individual~~As previously stated the simulation process can ran, independently of tskit, but is required when planning to analyze the genealogy.

2.2 Simulations

Simulations start with a ~~burn-in phase of 100~~burn in or calibration phase of 50,000 generations for $b = 1$, and 200,000 generations for $b = 0.5$ (Figure S1 and Table S1 for empirically sufficient number of calibration generations given for a recombination rate), to make sure full coalescence has occurred and a most-recent common ancestor is present. We consider that after this initial phase, the population is at an equilibrium state in terms of neutral diversity, including within the seed bank. After this phase, ~~selectively advantageous mutations are introduced one at a time~~ one selectively advantageous mutation is introduced at the predefined site. To study sweep signatures as well as the time it takes for sweep signatures to recover, simulations are run for several generations after fixation of the beneficial allele (up to ~~4~~16,000 generations after fixation).

Except when indicated otherwise, the population size is generally set to $N = 500$ individuals or $2N = 1,000$ ~~chromosomes~~haploid genomes. We specifically change population size when testing whether sweep signatures can be explained by simple size scaling, and use values of N of ~~1,000,~~ 2,000 ~~, 4,000 and 8,000~~ individuals with a germination rate of $b = 1$~~. Our~~ , corresponding to a seed bank of $b = 0.35$ ($N = 245$ diploid individuals) (Figure S9). Our focal seed bank setup is ~~in that case~~ that of a population of $N = 500$ individuals with a germination rate ~~$b = 0.35$~~$b = 0.35$ and dominance coefficient $h = 0.5$. The genome ~~map~~ sequence length is set to ~~10~~100,~~000. The neutral mutation rate μ is set at $5e-5$ per locus and to~~ 000 bp, 1MB or 10 MB. Neutral diversity is calculated based on the branch length, meaning that explicitly simulating mutation is not required. To check whether the strength of a sweep behaves in accordance to ~~expectation~~ expectations *i.e.* lower recombination rates result in wider sweeps, recombination rates ~~of $r = 5e-5$, $1e-5$ and $1e-4$ are tested . These rates were multiplied by the map length to get the respective random Poisson sampling rate~~ranging from 5×10^{-8} to $r = 10^{-7}$ are tested for all parameter sets. Simulations are run for the germination rate b ranging from 0.25 up to 1 (with $b = 1$ meaning no dormancy). The upper-bound number of generations m which is the maximum time that seeds can remain dormant (*i.e.* seeds older than m are removed from the population) is set at ~~100~~ 30 generations. Beneficial mutations have a selective coefficient ~~s_i from 0.01 to 10~~ $N_e^{b=1}s$ ranging from 0.1 to 100 and dominance h takes values ~~0, 0.5~~ 0.1, 0.5 and 1.1, representing recessive, co-dominant and overdominant beneficial mutations.

2.3 Statistics and sweep detection

We ~~calculate first~~ first calculate several statistics relative to the forward-in-time change of ~~advantageous allele frequency~~ the frequency of an advantageous allele in the population~~such as~~ , such as the mean time to fixation and the probability of fixation, using 1,000 simulations per parameter configuration.

Each simulation run ~~consist~~ consists of the recurrent introduction over time of an allele (mutant ~~in frequency 1/2N~~at frequency $1/2N$) which is either lost or fixed. When an allele is lost ~~a new allele is introduced at the same position, and this procedure is repeated until one allele reaches fixation at which time the simulation run stops~~and the simulation is conditioned on fixation a new simulation starts from a neutral genetic diversity background (see below for more details). An allele is considered to be fixed if it stays ~~a frequency~~ at a size of 2N for ~~50~~ m consecutive generations. ~~We store for~~ For each simulation run we store 1) the time it takes for the last introduced allele to reach fixation (time between allele introduction until fixation), and 2) the number of alleles which were introduced until one has reached fixation (yielding the probability of fixation of an allele per simulation run). The resulting times to fixation and fixation probabilities are calculated as the averages over the 1,000 simulation runs.

We also compute statistics on the underlying coalescent tree and ancestral recombination graph (ARG) such as time to the most recent common ancestor, linkage disequilibrium (r^2, ~~Hill and Robertson 1968~~ Hill and Robertson, 1968), as well as Tajima's π ~~(Nei and Li 1979~~and D (Tajima, 1983; Nei and Li, 1979; Tajima, 1989) over windows of size ~~50 (or~~ 5,000 (giving 200 windows for a ~~map length of 10,000~~sequence length of 1 MB). This allows us to analyse the effects of seed-dormancy on the amount of linkage disequilibrium and nucleotide diversity along the genome, as well as the footprint of a selective sweep on these quantities. *Tskit* functions are used for diversity and linkage disequilibrium calculations. Nucleotide diversity (π) is ~~normalized by the map interval length and~~ calculated based on the ~~polymorphic sites and not the~~ branch length. Sweeps are detected using ~~the Omega statistic~~ Omega and SweeD statistic, the first one quantifies the degree to which LD is elevated on both sides of the selective sweeps, as implemented and applied with OmegaPlus (~~Alachiotis et al. 2012~~) Alachiotis et al., 2012), while SweeD (Pavlidis et al., 2013) uses changes in SFS across windows to detect sweeps. A difficult issue in detecting selective sweeps is choosing the correct window size to perform the computations. ~~If the window is too large, the sweep can be missed, if the window is too narrow, the number of false-positives can be inflated.~~ It is documented that the optimal window size depends on the recombination rate and thus the observed amount of linkage disequilibrium (~~Alachiotis et al. 2012; Alachiotis and Pavlidis 2016~~Alachiotis et al., 2012; Alachiotis and Pavlidis, 2016). We ~~thus~~ use two different setups with different window sizes: –minwin ~~100~~ 2000 –maxwin ~~1000~~ 50000 and –minwin ~~50~~ 1000 –maxwin ~~100. The~~ 25000 . The window sizes refer to the minimum and maximum region used to calculate LD values between mutations. Importantly the –minwin parameter determines the sensitivity, meaning the degree to which false positives or false negatives (high –minwin values) are detected, while the –maxwin parameter determines run-time and memory requirements. A detailed graphical description can be found in the online OmegaPlus manual. In theory the larger window size is ~~based on~~ more appropriate for the model without dormancy ($b = 1$), and the narrower window size ~~is based on~~ for the model with dormancy ($b < 1$)~~,~~. For both cases, we set –grid 1000 –length ~~100000 parameters are set equally for both cases~~10 MB. SweeD is only tested using a –grid 1000 parameter. The statistic is computed for a sample size of ~~500~~ 100 over 400 simulations for each ~~recovery scenario~~sweep signature at mulitple generations after fixation (sweep recovery scenerios).

2.4 Code description and availability

Source code of the simulator and demonstration of the analysis can be found at ~~and . On a Intel(R) Core(TM) i7-9750H CPU @ 2.60GHz processor, CPU/Wall times for a single time to the most recent common ancestor simulation of $N = 500$ individuals (no burn-in period) took 19.5 ms/44.7s and 21 ms/2 min 6s for b=1.0 and b=0.5, respectively.Including burn-in periods of 100 000 generations with a succeeding selection phase(selection coefficient $s = 1$)modified the~~ `https://gitlab.lrz.de/kevin.korfmann/sleepy` and `https://gitlab.lrz.de/kevin.korfmann/sleepy-analysis`. A convenient feature of the simulator is the option to choose between switching the tree sequence recording on or off depending on the question, i.e. if analysing fixation time and probability of fixation it is unnecessary to record the tree sequence (or use a calibration phase). To analyse the sweep signatures, the simulation process has been divided into two phases to alleviate the large run-times ~~to 26.5 ms/3min 59s and 19.4 ms/4min 44s for b=1.0 and b=0.5~~of forward simulations. During the first phase, a tree sequence will be generated under neutrality and stored to disk. And in the second phase the neutral tree sequence is loaded and a parameter of interest is tested until fixation or loss. Additionally, if the simulation is conditioned on fixation, then the simulation can start again from the beginning of the second phase that will have been run for tree sequence calibration, saving the time.

Listing 1: Simplified, demonstrative Python code example for a simulation with and without selection. Tree sequence results are stored in a specified output directory and are loaded via *tskit* function for further processing or analysis of e.g. linkage disequilibrium or nucleotide diversity along the genome. A more detailed version with more parameters can be found in the example notebook at https://gitlab.lrz.de/kevin.korfmann/sleepy-analysis.

Simulations rely on regular simplification intervals for efficiency of the genealogy recording, yet the weak dormancy model requires keeping up to m generations in memory even for past individuals (seeds) which do not have offspring in the current generation~~after a simplification procedure~~. To make sure that this assumption is realized in the code, up to m generations are technically defined as leaf nodes, thus hiding them from the regular memory clean-up process. ~~Further~~Furthermore, the presence or absence of an allele with an associated selection coefficient needs to be retrievable, even under the influence of recombination, for all individuals up to m generations in order to determine the fitness value of the individuals. Therefore, recombination and selective alleles are tracked additionally outside of the *tskit* table data structure ~~to avoid building~~ allowing for option of running the simulation without the tree sequence~~from the tables at each generation. This would have been necessary to determine which individuals have a selective allele or not~~. Both of these model requirements, namely maintaining individuals which do not have offspring in the current generation (but potentially could have due to stochastic resuscitation of a seed) as well as the knowledge about the precise state of that given individual in the past, are reasons to choose our own implementation over the otherwise advisable option SLiM (~~Haller and Messer 2019~~Haller and Messer, 2019).

3 Results

3.1 Neutral coalescence

We first verify that our simulator accurately produces the expected coalescent tree in a population with a seed bank with germination parameter b and population size $2N$. To do so, we first compute the time to the most recent common ancestor (TMRCA) of a coalescent tree for a sample size $n = 500$. We find that ~~, as expected,~~ the coalescent trees are scaled by a factor ~~of~~ $\frac{1}{b^2}$ independently of the chosen recombination rate (Figure ~~??~~2a). The variance of the TMRCA decreases with increasing recombination rate due to lower linkage disequilibrium among adjacent loci, as expected under the classic Kingman coalescent with recombination (~~Hudson 1983~~Hudson, 1983). Moreover, we also find that decreasing the value of b ~~,~~(*i.e.* the longer seeds remain dormant~~,~~) decreases linkage disequilibrium (Figure ~~??~~2b). This is a direct consequence of the scaling of the recombination rate by $\frac{1}{b}$, because any plant above-ground can undergo recombination (and can be picked as a parent with a probability b backward in time). Therefore, we observe here two simultaneous effects of seed banks on the ARG: 1) the length of the coalescent tree and the time between coalescent events is increased by a factor $\frac{1}{b^2}$ meaning an increase in nucleotide diversity (under a given mutation parameter μ), and 2) a given lineage has a probability br to undergo an event of recombination backward in time. In other words, even if the recombination rate r is slowed down by a factor b (because only above-ground plants may recombine~~, as~~), since the coalescent tree is lengthened by a factor $\frac{1}{b^2}$ there are on average $\frac{1}{b}$ more recombination events per ~~coalescent tree~~chromosome. This property of the ARG was used in ~~Sellinger et al. 2019~~ Sellinger et al., 2019 to estimate the germination parameter using the Sequential Markovian Coalescent approximation along the genome.

3.2 Allele fixation under positive selection

We examine the trajectory of allele frequency of neutral and beneficial mutations, by computing the probabilities and times to fixation over ~~a large number of~~ 1000 simulations. As expected for the case without dormancy ($b = 1$), the probability of fixation of a beneficial allele increases with the strength of selection (Figure 3a). ~~The discrepancy between the mathematically expected time to fixation in this case (Figure 3a - gray line) is likely an artifact of choosing the population size to be 500 diploid individuals, in which genetic drift plays an important role. However, larger population sizes increase the simulation run time considerably, especially when taking the scaling factor of $\frac{1}{b^2}$ of the germination rate into account. Thus, we avoid increasing the population size due to technical time and memory constraints of such forward simulation and point out that our conclusions are not affected by this discrepancy. With dormancy, we also observe a positive correlation between selection coefficients and the probability of fixation, while we also observe much lower probabilities of fixation (than in the absence of dormancy). Furthermore, as selection increases, so does the difference in fixation probability between simulations with $b = 1$ and $b < 1$. However, the difference of fixation probability between the case $b = 1$ and $b < 1$ is larger for weak selection than for strong selection coefficients (Figure 3a). Indeed, we note that for the strongest selection coefficients, the fixation probability under seed bankis a fraction of that under $b = 1$, and that factor is higher than b (for~~

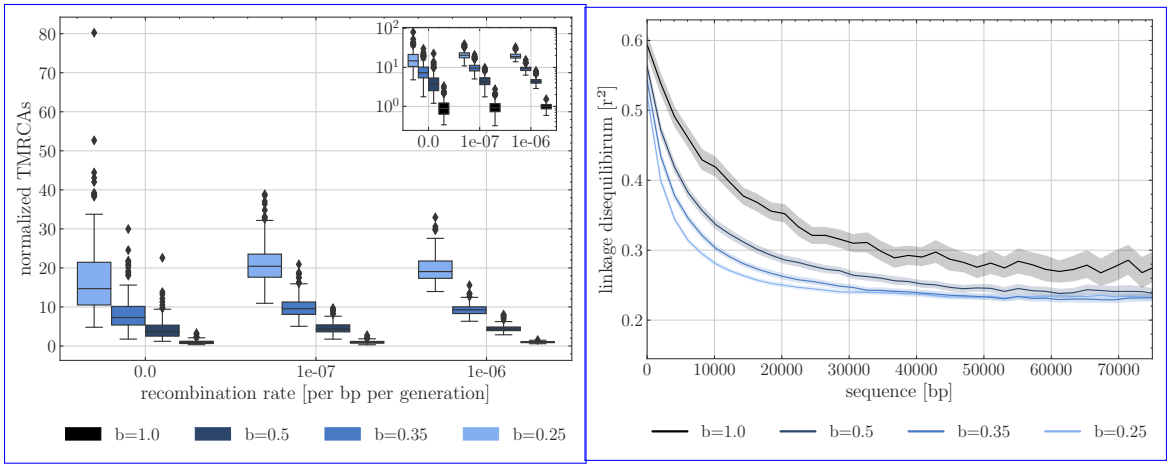

(a) **(b)**

Fig. 2. (a) Time to the most recent common ancestor (TMRCA) as a function of the germination rate b and scaled by ~~the~~ results under $b = 1$~~estimates taking diploidy into account~~. For each germination rate, three recombination rates per site are presented ($r = 0$, ~~$r = 1e-6$~~ $r = 10^{-7}$ and ~~$r = 5e-5$ from left~~ $r = 10^{-6}$. Boxes describe the 25th (Q1) to ~~right~~75th percentile (Q3), with the lower whisker representing Q1-1.5×(Q3-Q1) outlier threshold and the upper whisker is calculated analogously. The mean is plotted between Q3 and Q1. Each boxplot represents the distribution of 200 TMRCA values over 200 sequences of 0.1 Mb. Per sequence the oldest TMRCA is retained. (b) Monotonous decrease of linkage disequilibrium as a function of distance between pairs of SNPs, setting $r = 10^{-7}$ per generation per bp, sequence length to 10^5 bp. While population size is 500, linkage decay was calculated ~~using 50 equally spaced bins~~by subsetting 200 individuals, purely to constrain the computational burden. ~~Distance bin 10 represents two SNPs which are 10 distance bins apart~~In total 200 replicates were used for TMRCA and LD calculations.

~~example, at $s = 5$, the probability of fixation for $b = 1$ is approx. 1, and it is 0.55 for $b = 0.25$). For smaller selection coefficient, this factor decreases (for example, at $s = 1.5$~~

We note, that the mean fixation probability is unaffected by the seed bank, as when N_e is large enough and the coefficient of selection s is not too strong, the probability of fixation of ~~fixation for $b = 1$ is approx. 0.9, and it is 0.35 for $b = 0.25$~~a beneficial mutation depends only on hs (Barrett et al., 2006).

As expected from the neutral case, the time to fixation with dormancy becomes longer with smaller values of b (Figure 3b). When selection is weak ~~(*i.e.* selection coefficient 0.01)~~ the time to fixation is close to the expectation for neutral mutations (Figure 3c~~)~~, $b = 1$: $4N = 2000$ generations and $b = 0.25$: $4N \times \frac{1}{b^2} = 32,000$ generations). However, increasing s changes the scaling of the time to fixation. ~~Increasing the strength of selection tends to reduce the differences in times to fixationbetween the different germination rates. For strong selection, it becomes apparent that~~ Dormancy significantly increases the times to fixation~~are not scaled by a simple factor of $\frac{1}{b^2}$, which is the scaling for neutral mutations under dormancy. The latter observation that the time to fixation of strongly beneficial alleles, as well as for strongly deleterious alleles, does not scale with $\frac{1}{b^2}$ but rather almost as a linear function of b was already computed (Formula 19, Koopmann et al. 2017). However, the probability of fixation of beneficial alleles had not been addressed. Taken together,~~ , beyond that expected by N_e. This can be seen by comparing the expectations for the ~~results in Figure 3a, 3b and 3c demonstrate that the selection is slowed down by dormancy (Hairston Jr and De Stasio Jr 1988; Shoemaker and Lenno)and leads to many more mutations to occur and get lost. This is due to an increased time window for the loss of a mutation due to beneficial alleles remaining~~ times to fixation for the rescaled effective population size without dormancy (blue lines in 3c) to those obtained from our simulations (black lines). In order to understand this observation, we examine the time an allele under selection remains at given frequencies in the above ground population. The trajectory of an allele undergoing selection can be separated into three phases: two that are qualified as "stochastic", when the allele is at a very low or very high frequency, and one "deterministic", during which the frequency of the allele increases exponentially (see Kim and Stephan, 2002). As shown in Figures S2-4, we find that the proportion of time spent at very low ~~frequencies for a longer period of time, and thus being more subjected to loss by genetic drift (Figure 3a). However, when the beneficial allele reaches fixation, the time to fixation does not scale by the inverse of the square of the germination rate as for neutral alleles (as was expected in Shoemaker and Lennon 2018~~and very high frequencies increases with increasing selection and increasing b (it is unaffected by b when selection is weak *i.e.* $s = 0.0001$). This ~~effect becomes non-linearly more pronounced with stronger selection coefficients and stronger the seed bank (Figure 3c) , yielding the counter-intuitive result that dormancy enhances the efficiency of selection compared to genetic drift (Koopmann et al. 2017).~~

observation, along with generally shorter relative times spent in the deterministic phase (Figure S4) with increasing b, imply that the seed-bank contributes to increasing the duration of the stochastic phases, slowing down the selection process.

3.3 Footprints of selective sweep

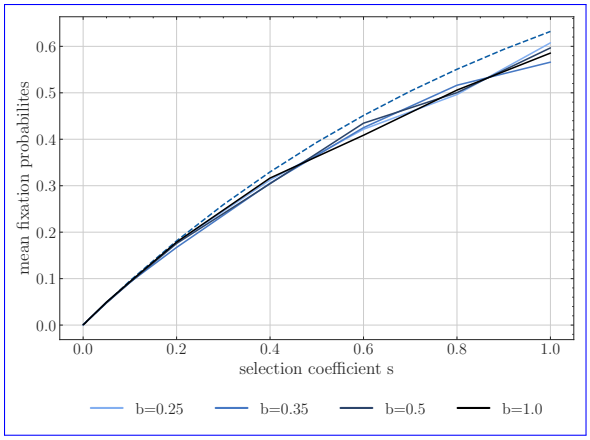

(a)

Fig. 3. (a) ~~Expected and simulated~~ Simulated estimates of the probability of fixation ~~: for germination rate~~ of ~~$b = 1$ for~~ an advantageous allele with different ~~selection~~ coefficients ~~, and simulated estimates~~ of selection s under absence of seed ~~dormancy fixation probabilities~~ bank $b = 1$ (black solid line) and various seed bank strength $b = 0.5, 0.35, 0.25$ (blue lines) along with ~~germination rate between $b = 0.25$ to $b = 1.0$~~the theoretical expectations for a neutral allele (dashed). (b) Time to fixation for different selection coefficients. Y-axis is the unnormalized time in generations, and X-axis is the germination rate ~~written as $\frac{1}{b}b$~~. (c) ~~Time~~ Normalized time to fixation with respect to $b = 1$ for ~~different~~ each selection ~~coefficients s normalized by~~ coefficient version of b). In b) and c) we indicate black lines for time to fixation under seed bank. The blue lines indicate the ~~expected~~ time to fixation in a population without dormancy but with ~~$b = 1$~~an effective population size scaled by $\frac{1}{b^2}$ and the respective scaled effective selection coefficient $N_e^b s$. ~~Y-axis is~~ For example, for $s = 0.001$, we quantify the fixation time ~~in generations~~ of alleles under $N_e^{b=1.0} s = 1$, $N_e^{b=0.71} s = 1.98$, $N_e^{b=0.5} s = 4$, $N_e^{b=0.35} s = 8.2$, and ~~X-axis~~ $N_e^{b=0.25} s = 16$ (indicated by the red vertical dashed lines). Population size is 500 diploids, $h = 0.5$, 1,000 replicates are used for each parameter combination, and shaded areas represent the ~~germination rate written as $\frac{1}{b}$~~95% confidence interval. Dashed-blue lines indicate theoretical expectations of a N_e-scaled population corresponding to a given seed bank strength.

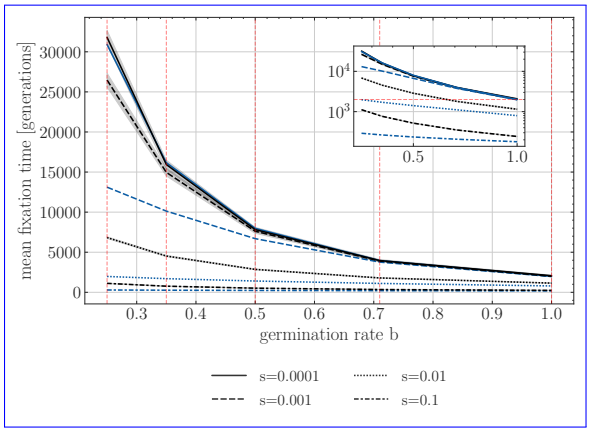

(b)

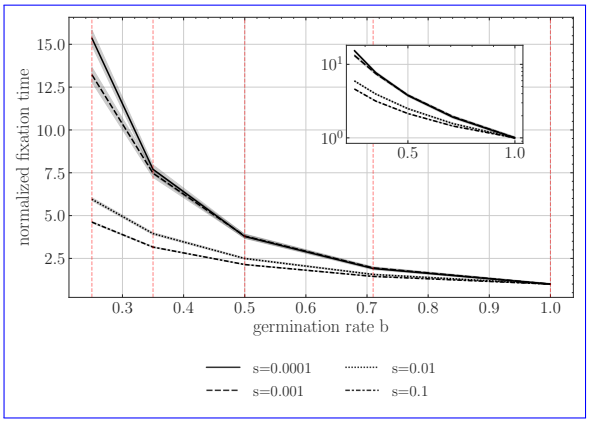

(c)

~~Following on the time and probability of fixation results, we now make use of~~ Now that we have a clearer indication of the dynamics of allele fixation, we use our new simulation tool to investigate the genomic diversity and signatures of selective sweeps at and near the locus under positive selection by simulating long portions of the genome (Figure ~~??~~4). In accordance with the results from Figures ~~??~~ 2a and 2b and the effects of the seed bank in maintaining genetic diversity, smaller germination rates lead to higher neutral genetic diversity due to the lengthening of the coalescent trees (e.g. Figure 4a measured as Tajima's π). Moreover, stronger dormancy ~~generates also~~ also generates narrower selective sweeps around sites under positive selection which have reached fixation ~~, in~~ S10. In other words, there is a narrower genomic region of hitch-hiking effect around the site under selection (~~Maynard Smith and Haigh 1974~~Maynard Smith and Haigh, 1974). This is due to the re-scaling of the recombination rate as a consequence of dormancy (e.g. Figure ~~4a and 4c~~4b, 4d and S10). We note that with lower germination rates the depth of the sweeps increases in absolute diversity ~~term~~ terms (Figure 4a) but not in relative diversity (Figure ~~4c) with lower germination rates, due to 1)the higher diversity under dormancy, and 2) the increased efficacy of selection compared to drift at the site under selection~~4b), when scaling by $\frac{1}{b^2}$. However, we observe that nucleotide diversity close to the site under selection is not zero (Figure 4a) because of the longer times to fixation of a positive mutation and longer time for drift and new ~~mutation~~ mutations to occur at neutral alleles close to the selected site. The results in Figure ~~??~~ 4 reflect the manifold effect of dormancy on neutral and selected diversity as well as recombination rate (Figures ~~??~~ 2b and 3c). Furthermore, as recombination and selection are scaled by different functions of the germination rate, the results in Figure ~~??~~ 4 cannot be produced by scaling ~~only the~~ by the expected effective population size in the absence of dormancy ~~. We present different simulations with population sizes in the absence of dormancy and show that these do not produce the footprint of selective sweep under dormancy ($b = 0.35$, Figure 4d~~(Figure S9), since that would likewise scale the recombination rate by $\frac{1}{b^2}$, when it should be only scaled by $\frac{1}{b}$. Scaling only by the effective population size, leads to narrower sweeps in the $b = 1$ model (Figure S9). Additionally, seed bank diversity appears to ~~increase~~ decrease visibility of the sweep when ~~a strong dominance coefficient~~ mutations are overdominant ($d = 1.1$ with $b = 0.35$, ~~Appendix Figure 2) is associated with the selective allele~~ Figure S6) due to the increased ~~efficacy of selection under dormancy~~time over which recombination can act to reduce linkage within the region. We finally point out that while the signatures of sweeps appear sharp in Figure ~~??~~4, it is because these are averaged footprints over ~~100~~ 400 repetitions. Each ~~individual simulation produces variance in~~ simulation shows variance in both nucleotide diversity and ~~of~~ the sweep signature~~which conditions~~ , both of which condition the detectability of the sweep against the genomic background.

3.4 Detectability of selective sweeps

~~As a result of~~ Based on the previous results, we hypothesize that, compared to the absence of seed banking, the detectability of selective sweeps in a species with seed bank is affected 1) in the genome space, that is the ability to detect the site under selection, and 2) in time, that is the ability to detect a sweep after the fixation of the beneficial allele. First, as the footprints of selective sweeps are sharper and narrower in the genome under a stronger seed bank, we expect that the detection

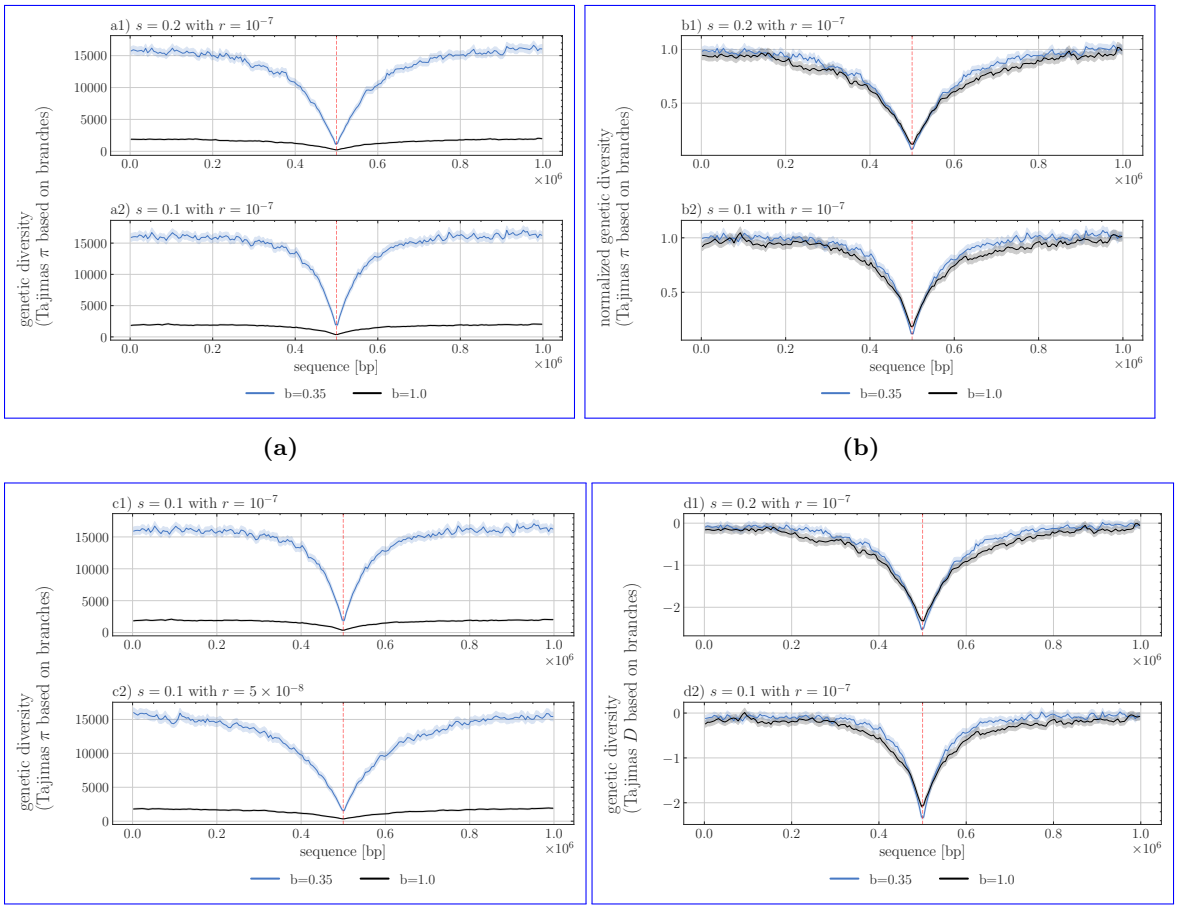

Fig. 4. ~~Nucleotide~~ Signature of selective sweeps as measured by nucleotide diversity (~~Tajima's~~ Tajimas π in a, ~~Y-axis~~b, c) and Tajimas D (in d) over ~~map~~ 1Mb sequence length (X-axis)~~for sliding~~, the selected site being located in the middle of the segment. The statistics are computed per windows of size ~~50 mapping length~~ 5,000 bp and averaged over ~~100~~ 200 repetitions, the shaded area representing the 95% confidence interval. The black line indicates the value in absence of seed bank (~~A) Comparison between germination rate~~ $b = 1$ ~~and~~), the blue line with dormancy ($b = 0.35$ ~~for~~). a) π assuming two selection coefficients ~~$s = 0.5$~~ $N_e^{b=1}s = 200$ (a1) and ~~$s = 2.0$~~ $N_e^{b=1}s = 100$ (a2) with $h = 0.5$. (~~B~~b) Normalized ~~nucleotide diversity (π) computed~~ as ~~the diversity of the respected seed dormancy and selection coefficient combinations~~ divided by the ~~mean~~ average neutral branch diversity ~~of map length at position 0-1~~from (a) using the values 2,000 and ~~9~~16,~~000-10~~000 for $b = 1$ and $b = 0.35$, ~~000.~~ respectively. (~~C~~c) ~~Effect of varying recombination~~ Recombination rates varies with values ~~$r = 10^{-4}$ and $r = 10^{-5}$ with~~ b1) $r = 10^{-7}$ per bp per generation and ~~without dormancy~~b2) $r = 5 \times 10^{-8}$ per bp per generation. (~~D~~d) ~~Comparison of footprints of selective sweeps under different population sizes N=1,000; 2,000; 4,000 and 8,000 without dormancy with~~ Tajimas D based on simulations from a ~~selective sweep under germination rate of $b = 0.35$~~and b.

of these sweeps likely requires adapting the different parameters of sweep detection tools, namely the window size to compute sweep statistics. Second, in a population without dormancy, the time for which the detection of a selective sweep signature is possible is approximately 0.1N generations (~~Kim and Stephan 2002~~Kim and Stephan, 2002). We hypothesize that as the ~~rate of mutation~~ mutation rate and genetic drift ~~is~~ are scaled by $1/b^2$, the time it takes a sweep to recover after it has reached the state of fixation is slowed down. The time window for which a sweep could still be detected would then be potentially longer than ~~0.1N~~ $0.1N$ generations.

In Figure 5 we show the results obtained using OmegaPlus ~~, a tool~~ and SweeD, both tools for detecting selective sweeps ~~Alachiotis et al. 2012~~(Alachiotis et al., 2012; Pavlidis et al., 2013). As noted above, ~~detection of a sweep~~ individual simulations show significant variation in nucleotide diversity and LD, which is not captured by the mean diversity over several runs plotted in the figures above. As the detection of sweeps is performed against the genomic background ~~(nucleotide diversity, amount of LD) which varies for~~ of each individual simulation~~more than apparent in the above figures which are averages over several repetitions. This~~ , this variation in nucleotide diversity and LD ~~along a chromosome generates~~ generate confounding effects and define the rates of false positives expected from the detection test.

We find that when using the same large detection window "–minwin ~~100~~ 2000 –maxwin ~~1000~~50000" for $b = 1$ and $b = 0.35$ (Figures ~~5a and 5b~~5 a21 and 5 b21), sweep detection almost completely fails for ~~$b = 0.35$ (Figure 5b). Based on neutral simulations, we choose a threshold for detection of 2, 000 for the case without seed bank (Figure 5a), in order to~~ $b = 1$, unless the fixation has just occurred, meaning that no generation has passed since the fixation event. For $b = 0.35$ sweeps are detectable up to >2000 generations after fixation. Following the classic procedure to detect sweeps, we use neutral simulations to define different thresholds for detection which obtain a false positive rate of less than ~~0.1 and a detection power of approximately 85% of sweeps. Under this large window setting, we require a much smaller threshold (<500) when $b = 0.35$ only to obtain approximately 30% of sweeps detected. Without dormancy, the detectability of sweep is very low (approx. 25%) already 500 generations after the fixation event (Figure 5b, with a threshold of~~ 0.05. Decreasing the window size is generally associated with a loss of sensitivity, increasing the rate of false positives. This is true for $b = 1$ (see neutral threshold line in Figure 5 b21 and b22), indicating a decrease from roughly 60 % detected sweeps to 40 % (after 400 repetitions). However, older sweeps of >2,000 ~~). However, when decreasing the window size to "–minwin 50 –maxwin 100" in Figure ?? and ??, the detectability of sweeps is largely increased under seed banking (Figure ??), while becoming worst in the absence of seed bank (Figure ??). When setting a threshold of 300 in Figure ??, about 85% of the sweeps can be detected at the time of fixation, and about 40-50% of sweeps as old as 500 up to 1~~generations become detectable for $b = 0.35$ (Figure 5 b22). Results using SweeD support this increased detectability, also when using the SFS statistics, showing the possibility of locating sweeps approximately up to 2,000 generations ~~can be detected. We here note the~~ after fixation (Figure 5 a3 and b3)

We note that there is a much sharper decrease in the rate of detection of false positive sweeps (neutral simulation line in Figure 5) under seed bank compared to the absence of a seed bank. Lastly, the possibility to locate sweeps multiple generations after the fixation event emphasizes the slower

recovery of nucleotide diversity post-fixation in combination with the already established narrowness of the signature in the presence of a seed bank for a given population size N ($b = 0.35$, ~~Appendix Figure 1~~Figure S5).

4 Discussion

We investigate the neutral and selective genome-wide characteristics of a weak seed bank model by means of a newly developed simulator. We first characterize the emergent behavior of an adaptive allele under a weak seed bank model, ~~providing estimations of~~ and simulate the times to and probabilities of fixation, considering different strengths of selection and recombination. In populations without seed banks, a neutral mutation is expected to fix after a ~~period of $\frac{1}{2N_e}$ generations and $\approx \frac{1}{2N_e s}$~~ time of $2N_e$ generations and $\approx 2N_e s$ if the allele is under ~~selection (Kimura 1962~~ weak selection (Kimura, 1962). Though both processes are re-scaled by the weak dormancy model (~~Koopmann et al. 2017~~Koopmann et al., 2017), the time to fixation of a neutral mutation ~~is lengthened by a factor b^2 (as~~ can be obtained by rescaling N_e appropriately ($N_e = \frac{N}{b^2}$ in the case of a seed bank, with b the germination rate)~~but the scaling in the event of selection is not as simple to determine. Under~~. This remains true under weak selection, however under strong selection the time to fixation is ~~increased by a function approximately linear in b (Koopmann et al. 2017), while under weak selection, the factor is again $\frac{1}{b^2}$. Importantly, when computing the fixation probability for beneficial alleles, we also observe a non-linear effect of germination rate b depending on the selection coefficient. We conclude that~~ significantly decreased and cannot be explained by the change in N_e alone. In accordance with existing theory, the probability of fixation is unaffected by the seed bank ~~magnifies (respectively decreases)the efficacy of selection compared to genetic drift for strong (respectively small) selection coefficients~~(since it depends only on sh, see for example Barrett et al., 2006), implying that the main effect of seed banks is on the dynamics of allelic frequencies, but not on the outcome of selection at a single locus. Combining this observation and the effect of seed banks on increasing the effective recombination rate, we ~~find~~ suggest that the signatures of sweeps ~~are~~ may be slightly easier to detect in the presence of seed banking as shown by the sharpness and depth of the nucleotide diversity pattern (the so-called valley of polymorphism due to genetic hitch-hiking, ~~Maynard Smith and Haigh 1974; Kim and Stephan 2002~~ Maynard Smith and Haigh, 1974; Kim and Stephan, 2002) against the genomic background.

4.1 Dynamics of alleles under positive selection

Our results regarding the time to fixation of advantageous alleles are in line with previous works ~~(Hairston Jr and De Stasio Jr 1988; Koopmann et al. 2017; Heinrich et al. 2018; Shoemaker and Lennon 2018)~~ in showing that a weak seed bank delays the time to fixation (Hairston Jr and De Stasio Jr, 1988; Koopmann et al., 2017). However, a novelty here is that we refine these results in showing that the time to fixation of a weakly ($~~s < 1~~s < 0.01$) and a strongly ($~~s >= 1~~s \geq 0.01$) positively selected allele differ under seed bank: the selection on weak alleles is delayed by a factor $\frac{1}{b^2}$ while ~~the strong selection~~for strong selection, the time to fixation is delayed by ~~a factor close to $\frac{1}{b}$~~ more than would be expected for

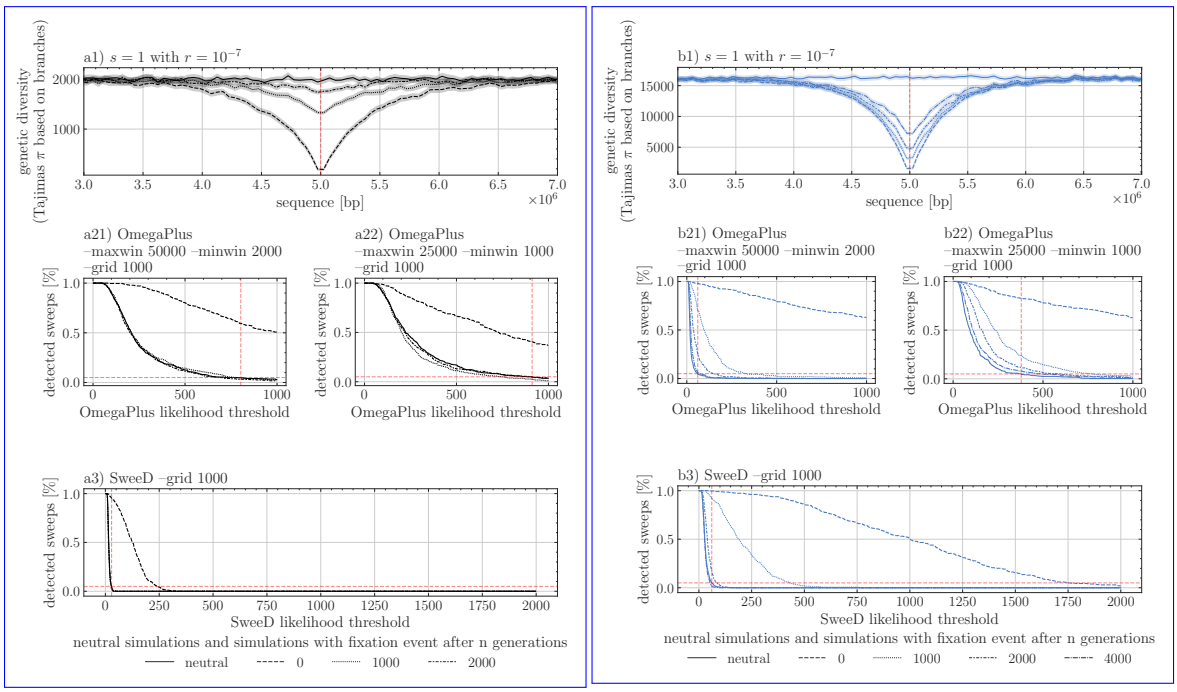

(a) **(b)**

Fig. 5. Selective sweep detection depending on the threshold of OmegaPlus or SweeD statistics on a 10MB sequence with a strong selective mutation of $N_e^{b=1}s = 1{,}000$ located in the middle of the sequence. Two germination rates apply: a1) $b = 1$ and b1) $b = 0.35$, with the signature of sweep being shown at various time points after the fixation event (1000, 2000 and 4000 generations). Results for two window sizes "–minwin 2000 –maxwin 50000" (a12,b12) and "–minwin 1000 –maxwin 25000" (a22,b22) for analysis with OmegaPlus and SweeD (a3 and b3) using a grid size of 1,000. The percentage of detected sweeps is indicated for a given user-defined threshold value on the X-axis. Vertical dashed lines indicate the 5% sweep detection based on neutral simulations, setting up the false positive rate. Recombination rate is $r = 1 \times 10^{-7}$ per bp per generation for all sweep simulations, and 400 replicates for each parameter.

~~Selective sweep detectability depending on the threshold of OmegaPlus statistics. Results for two window sizes " minwin 100 –maxwin 1000" (a,b) and " minwin 50 –maxwin 100" (c,d) and without seed bank (a, c) and under germination rate of $b = 0.35$ (b, d), the lines indicate the time since fixation of the beneficial allele (time to fixation up 2,000 generations after fixation). The neutral simulation line represents the false positive rate of detection expected at a given threshold value of the statistics based on a sample size of 500 for 400 simulations. A selection coefficient of $s = 1.0$ and recombination rate $r = 5 \times 10^{-5}$ was set for all sweep simulations.~~

a population without a seed bank but the same effective population size(see Figure 3b,3c~~). The analytical formula is found in Koopmann et al. 2017, though this model assumes~~ , and Koopmann et al. 2017 for an analytical approach with an infinite deterministic seed bank~~. Moreover, we provide a second new result (Figure 3a): the probability of allele fixation as a function of the germination parameter and selection coefficient. Interestingly, the probability~~). We show that this delay can be explained by an increase in the time spent in the stochastic phases of allele fixation ~~becomes lower with a longer seed bank, though there is a complex non-linear interaction between the germination rate and the selection coefficient~~(at below 10% and above 90% in the above ground population). In other words, ~~as a~~ the seed bank delays the action of selection under the weak seed bank model (due to the dormant compartment acting as a buffer slowing down allele frequency change)~~, genetic drift has more time to act and advantageous alleles may be lost. This is especially true in~~ . In the initial phase of selection when the advantageous allele is at a very low frequency in the (active) population, before reaching the phase of exponential allele frequency increase (which is almost deterministic, ~~Kim and Stephan 2002~~Kim and Stephan, 2002). This delay in the initial selection phase is visible in Figure 4a in ~~Shoemaker and Lennon 2018~~Shoemaker and Lennon, 2018. Our results are valid for the weak seed bank model (likely realistic for plants and invertebrates, as studied in Figure 4a in ~~Shoemaker and Lennon 2018, and Koopmann et al. 2017~~Shoemaker and Lennon, 2018 , and Koopmann et al., 2017) and we find that there exists a unique phase of selection encompassing the time until all individuals (in the active and dormant population) have fixed the advantageous allele. Strong seed bank models behave differently with respect to time to fixation of alleles under selection (~~Shoemaker and Lennon 2018~~Shoemaker and Lennon, 2018), showing two distinct phases: a first rapid phase of selection in the active population, followed by a second long delay until there is fixation in the dormant population. We are not aware of any results regarding the effect of strong seed banking on the probability of allele fixation. Our results ~~suggest that the paradigm~~ thus mitigate the previous claim that (weak) seed banks ~~enhance the effect of selection against drift (Koopmann et al. 2017; Shoemaker and Lennon 2018; Živković and Tellier 2018) is only valid for strong selection (high coefficients of selection) but not for weak selection. This implies that although seed banks~~ may amplify selection, making it relatively more efficient with regards to the effects of genetic drift which did not compute the probability of fixation of an advantageous allele. Longer times to fixation should promote genetic diversity, ~~this~~ but as the probability of fixation at a single locus is unchanged by the seed bank, dormancy does not necessarily ~~equate with enhanced adaptive potential~~ enhance the adaptive potential (by positive selection) of a population.

4.2 Signals of selective sweeps

~~When selection is strong enough to overcome genetic drift, resulting in allele fixation, we can study its footprints in the genome.~~ The precise signature of a positive selective sweep is dependent on a variety of factors, *i.e.* age of the observation after fixation, degree of linkage due to recombination, and its detectability depends on the specified window size to compute polymorphism statistics. However, in the case of sweeps under seed bank, two effects are at play and change the classic expectations based on the hitch-hiking model without generation overlap. First, as

the effective population size under seed bank increases with smaller values of b, an excess of new mutations is expected to occur after fixation around the site under selection compared to the absence of seed bank. As these new mutations are singleton SNPs, we suggest that the signature of selective sweeps observed in the site-frequency spectrum (U-shaped SFS) should be detectable under seed bank (~~Maynard Smith and Haigh 1974; Kim and Stephan 2002). This effect should be detectable by~~ Maynard Smith and Haigh, 1974; Kim and Stephan, 2002). Additionally, this effect was also detectable by the other sweep detection methods based on the SFS ~~such as SweeD (CLR test, Pavlidis et al. 2013), a key point is that the genomic windows for CLR statistics have to be decreased due to the presence of seed bank, yet, they should contain enough SNPs~~(SweeD, Pavlidis et al., 2013), finding sweeps older than 2000 generations (for N=500).

Second, the signature of sweeps also depends on the distribution of linkage disequilibrium (LD) around the site under selection (~~Alachiotis et al. 2012; Bisschop et al. 2021~~Alachiotis et al., 2012; Bisschop et al., 2021), which is affected by the seed bank (Figure ~~??~~4). Theoretically, it has been shown that patterns of LD both on either side and across the selected site generally provide good predictive power to detect the allele under selection. We use this property when using OmegaPlus, which relies on LD patterns across sites. Further past demography should be accounted to correct for false positives, due for example to bottlenecks (see review in ~~Stephan 2019~~Stephan, 2019). We speculate that a high effective recombination rate around the site under selection, as a consequence of the seed bank, maybe an advantage when detecting sweeps. This allows the avoidance of confounding effects due to the SFS shape, which is sensitive to demographic history. We also highlight that the narrower shape of the selective sweep under stronger seed bank, and the smaller number of loci contained in the window, reduce the number of false positives.

As mentioned above, a crucial parameter to detect sweeps is the window length to compute the statistics that the various methods rely on. The optimal window size depends on the neutral background diversity around the site of interest, which is a consequence not only of the rate of recombination but also the scaled rate of neutral mutations. We choose a constant mutation rate over time, and make the assumption of mutations being introduced during the dormant phase (in the seeds) at ~~a constant rate as well~~ this constant rate (see equations in introduction). This simplifying assumption is partially supported by empirical evidence (~~Levin 1990; Whittle 2006; Dann et al. 2017~~ Levin, 1990; Whittle, 2006; Dann et al., 2017), and has so far been made in the wider field of inference models, notably in the ecological sequential Markovian coalescent method (eSMC, ~~Sellinger et al. 2019~~ Sellinger et al., 2019). While assuming mutation in seeds favors the inference of footprints of selection by simply adding additional data, which subsequently increases the likelihood to observe recombination events, it remains unclear if this assumption is justified for all plant species and/or if mutations occur at a different rate depending on the age of seeds. More research on the rate of mutation and stability of DNA during dormant phases is needed in plant (*e.g.*~~Waterworth et al. 2016~~ Waterworth et al., 2016) and invertebrate species. Nevertheless, even if this mutation rate in seeds is relatively low, our results of a stronger signal of selection under seed banking than in populations without seed banking are still valid. In contrast to the weak seed bank model, it is possible to test for the existence of mutations during the dormant stage under a strong seed bank model as assumed in prokaryotes, because of the much longer dormant phase compared to the coalescent

times (~~Blath et al. 2020~~Blath et al., 2020).
Finally, as for all sweep models, we show that selective events that are too far back in the past cannot be detected under seed banks. Nonetheless, we show that when there is a seed bank, older sweeps can be detected with ~~decent~~ increasing accuracy. The presence of a long persistent seed bank could therefore be convenient when studying older adaptation events in plants and invertebrates that have some form of dormancy. This prediction also agrees with the previous observation that the footprint of older demographic events is stored in the seed bank (predicted in ~~Živković and Tellier 2012~~Živković and Tellier, 2012, observed theoretically in ~~Sellinger et al. 2019, and empirical example in Daphnia Möst et al. 2015~~Sellinger et al., 2019, and empirically observed in *Daphnia* in Möst et al., 2015). Our results open avenues for further testing the correlation between past demographic events and selective events for species that present this life-history strategy. However, current methods estimating the age of selective sweeps (~~McSwan, Tournebize et al. 2019; Bisschop et al. 2021~~ Tournebize et al., 2019; Bisschop et al., 2021) would need to use an *ad hoc* simulator (*e.g.* such as the one we present here) to generate neutral and selected simulations under seed banking.

4.3 Strengths and limitations of the simulation method

The simulation program developed and used in this work, written in C++, is centered on the use of *tskit*. The toolkit allows for the efficient storage of genealogies through time, by removing lineages that have effectively gone extinct in the current population, thus simplifying the genealogy at regular intervals during the program run-time. Despite all our efforts to streamline the process, forward simulations are inherently limited, because each generation has to be produced sequentially. Thus, while being more flexible and intuitively easier to understand than their coalescent counterparts, forward simulations sacrifice computational efficiency in terms of memory and speed. While simulating hundreds or thousands of individuals is possible (also storing their genealogies in a reasonable amount of time), this limitation becomes exaggerated when adding genomic phenomena such as recombination, and even more so when considering ecological characteristics such as seed banking. The latter scales the process of finding the most recent common ancestor by an inverse factor of b^2. As this leads to an increase in run-time of the order of ~~$O(n^2)$~~$O(1/b^2)$, we kept the population size at 500 (hermaphroditic) diploid individuals. ~~Further~~Furthermore, the output format of the simulations are tree sequences, which enables downstream processing and data analysis without the elaborate design of highly specific code. We believe that our code is the first to allow simulations of long stretches of DNA under the seed bank model including recombination and selection. In a previous study, we developed a modified version of the neutral coalescent simulator ~~scrm (Staab et al. 2015~~*scrm* (Staab et al., 2015) which includes a seed bank with recombination (~~Sellinger et al. 2019~~Sellinger et al., 2019). Our current simulator can be used to study the effect and signatures of selection along the genome under dormancy for non-model species such as plants or invertebrates with reasonably small population sizes.

4.4 Towards more complete scenarios of selection

We here explore a scenario in which a single beneficial allele is introduced. The much longer times to fixation in the presence of seed banks suggest that such a scenario may be unlikely. Indeed, it is probable that several alleles under selection, potentially affecting the same biological processes, are maintained simultaneously in populations for longer periods of time. We can therefore surmise that under seed banking, polygenic selective processes and/or competing selective sweeps, often associated with complex phenotypes and adaptation to changing environmental conditions in space and time, should be common.

From the point of view of genomic signatures of selection, the overall effectiveness of selection at a locus coupled with increased effective recombination with seed banking generate narrower selective sweeps, hence less genetic hitch-hiking throughout the genome. While we show that these effects can be advantageous to detect selective sweeps, we speculate that this might not be the case for balancing selection. If seed banks do promote balancing selection (~~Tellier and Brown 2009~~ Tellier and Brown, 2009), the expected genomic footprints would be likely narrowly located around the site under selection, and the excess of nucleotide diversity would not be significantly different from the rest of the genome. The presence of seed banking would therefore obscure the signatures of balancing selection. Concomitantly, the Hill-Robertson-Effect and background selection are expected to be weaker under longer seed banks. These predictions could ultimately define the relationship between linkage disequilibrium, the efficacy of selection and observed nucleotide diversity in species with seed banks compared to species without it (~~Tellier 2019, Živković and Tellier 2018~~Tellier, 2019 , Živković and Tellier, 2018).

Acknowledgements

The authors gratefully acknowledge the computational and data resources provided by the Leibniz Supercomputing Centre (www.lrz.de). KK is supported by a grant from the Deutsche Forschungsgemeinschaft (DFG) through the TUM International Graduate School of Science and Engineering (IGSSE), GSC 81, within the project GENOMIE QADOP. AT receives funding from the Deutsche Forschungsgemeinschaft (DFG) grant TE809/1-4, project 254587930. DAA was a Humboldt Post-Doctoral fellow.

Conflict of interest disclosure

The authors declare that they have no financial conflict of interest with the content of this article.

References

N. Alachiotis and P. Pavlidis. Scalable linkage-disequilibrium-based selective sweep detection: a performance guide. *GigaScience*, 5:7, 2016. ISSN 2047-217X. doi: 10.1186/s13742-016-0114-9.

N. Alachiotis, A. Stamatakis, and P. Pavlidis. OmegaPlus: a scalable tool for rapid detection of selective sweeps in whole-genome datasets. *Bioinformatics*, 28(17):2274–2275, Sept. 2012. ISSN 1460-2059, 1367-4803. doi: 10.1093/bioinformatics/bts419. URL https://academic.oup.com/bioinformatics/article-lookup/doi/10.1093/bioinformatics/bts419.

R. D. H. Barrett, L. K. M'Gonigle, and S. P. Otto. The Distribution of Beneficial Mutant Effects Under Strong Selection. *Genetics*, 174(4):2071–2079, 12 2006. ISSN 1943-2631. doi: 10.1534/genetics.106.062406. URL https://doi.org/10.1534/genetics.106.062406.

G. Bisschop, K. Lohse, and D. Setter. Sweeps in time: leveraging the joint distribution of branch lengths. *Genetics*, 219(2):iyab119, Oct. 2021. ISSN 1943-2631. doi: 10.1093/genetics/iyab119.

J. Blath, A. González Casanova, B. Eldon, N. Kurt, and M. Wilke-Berenguer. Genetic Variability Under the Seedbank Coalescent. *Genetics*, 200(3):921–934, July 2015. ISSN 1943-2631. doi: 10.1534/genetics.115.176818.

J. Blath, A. G. Casanova, N. Kurt, and M. Wilke-Berenguer. A NEW COALESCENT FOR SEED-BANK MODELS. *The Annals of Applied Probability*, 26(2):857–891, 2016. ISSN 1050-5164. URL https://www.jstor.org/stable/43859616.

J. Blath, E. Buzzoni, A. González Casanova, and M. Wilke-Berenguer. Structural properties of the seed bank and the two island diffusion. *Journal of Mathematical Biology*, 79(1):369–392, July 2019. ISSN 1432-1416. doi: 10.1007/s00285-019-01360-5. URL https://doi.org/10.1007/s00285-019-01360-5.

J. Blath, E. Buzzoni, J. Koskela, and M. Wilke Berenguer. Statistical tools for seed bank detection. *Theoretical Population Biology*, 132:1–15, Apr. 2020. ISSN 00405809. doi: 10.1016/j.tpb.2020.01.001. URL https://linkinghub.elsevier.com/retrieve/pii/S0040580920300010.

J. H. Brown and A. Kodric-Brown. Turnover Rates in Insular Biogeography: Effect of Immigration on Extinction. *Ecology*, 58(2):445–449, 1977. ISSN 0012-9658. doi: 10.2307/1935620. URL https://www.jstor.org/stable/1935620.

D. Cohen. Optimizing reproduction in a randomly varying environment. *Journal of Theoretical Biology*, 12(1):119–129, Sept. 1966. ISSN 0022-5193. doi: 10.1016/0022-5193(66)90188-3. URL https://www.sciencedirect.com/science/article/pii/0022519366901883.

M. Dann, S. Bellot, S. Schepella, H. Schaefer, and A. Tellier. Mutation rates in seeds and seed-banking influence substitution rates across the angiosperm phylogeny. Technical report, bioRxiv, June 2017. URL https://www.biorxiv.org/content/10.1101/156398v1. Type: article.

M. E. K. Evans and J. J. Dennehy. Germ banking: bet-hedging and variable release from egg and seed dormancy. *The Quarterly Review of Biology*, 80(4):431–451, Dec. 2005. ISSN 0033-5770. doi: 10.1086/498282.

N. G. Hairston Jr and B. T. De Stasio Jr. Rate of evolution slowed by a dormant propagule pool. *Nature*, 336(6196):239–242, Nov. 1988. ISSN 1476-4687. doi: 10.1038/336239a0. URL https://www.nature.com/articles/336239a0.

B. C. Haller and P. W. Messer. SLiM 3: Forward Genetic Simulations Beyond the Wright-Fisher Model. *Molecular Biology and Evolution*, 36(3):632–637, Mar. 2019. ISSN 1537-1719. doi: 10.1093/molbev/msy228.

L. Heinrich, J. Müller, A. Tellier, and D. Živković. Effects of population- and seed bank size fluctuations on neutral evolution and efficacy of natural selection. *Theoretical Population Biology*, 123:45–69, Sept. 2018. ISSN 0040-5809. doi: 10.1016/j.tpb.2018.05.003. URL https://www.sciencedirect.com/science/article/pii/S0040580917301715.

W. G. Hill and A. Robertson. Linkage disequilibrium in finite populations. *TAG. Theoretical and applied genetics. Theoretische und angewandte Genetik*, 38(6):226–231, June 1968. ISSN 0040-5752. doi: 10.1007/BF01245622.

R. R. Hudson. Properties of a neutral allele model with intragenic recombination. *Theoretical Population Biology*, 23(2):183–201, Apr. 1983. ISSN 0040-5809. doi: 10.1016/0040-5809(83)90013-8.

I. Kaj, S. M. Krone, and M. Lascoux. Coalescent theory for seed bank models. *Journal of Applied Probability*, 38:285–300, 2001.

J. Kelleher, K. R. Thornton, J. Ashander, and P. L. Ralph. Efficient pedigree recording for fast population genetics simulation. *PLOS Computational Biology*, 14(11):e1006581, Nov. 2018. ISSN 1553-7358. doi: 10.1371/journal.pcbi.1006581. URL https://journals.plos.org/ploscompbiol/article?id=10.1371/journal.pcbi.1006581.

Y. Kim and W. Stephan. Detecting a local signature of genetic hitchhiking along a recombining chromosome. *Genetics*, 160(2):765–777, Feb. 2002. ISSN 0016-6731. doi: 10.1093/genetics/160.2.765.

M. Kimura. On the Probability of Fixation of Mutant Genes in a Population. *Genetics*, 47(6):713–719, June 1962. ISSN 0016-6731. URL https://www.ncbi.nlm.nih.gov/pmc/articles/PMC1210364/.

B. Koopmann, J. Müller, A. Tellier, and D. Živković. Fisher–Wright model with deterministic seed bank and selection. *Theoretical Population Biology*, 114:29–39, Apr. 2017. ISSN 0040-5809. doi: 10.1016/j.tpb.2016.11.005. URL https://www.sciencedirect.com/science/article/pii/S0040580916301009.

J. T. Lennon, F. den Hollander, M. Wilke-Berenguer, and J. Blath. Principles of seed banks and the emergence of complexity from dormancy. *Nature Communications*, 12(1):4807, Aug. 2021. ISSN 2041-1723. doi: 10.1038/s41467-021-24733-1.

D. A. Levin. The Seed Bank as a Source of Genetic Novelty in Plants. *The American Naturalist*, 135(4):563–572, 1990. ISSN 0003-0147. URL https://www.jstor.org/stable/2462053.

F. Manna, R. Pradel, R. Choquet, H. Fréville, and P.-O. Cheptou. Disentangling the role of seed bank and dispersal in plant metapopulation dynamics using patch occupancy surveys. *Ecology*, 98(10):2662–2672, Oct. 2017. ISSN 0012-9658. doi: 10.1002/ecy.1960.

J. Maynard Smith and J. Haigh. The hitch-hiking effect of a favourable gene. *Genetics Research*, 23(1):23–35, Feb. 1974. ISSN 1469-5073, 0016-6723. doi: 10.1017/S0016672300014634. URL \url{https://www.cambridge.org/core/journals/genetics-research/article/hitchhiking-effect-of-a-favourable-gene/918291A3B62BD50E1AE5C1F22165EF1B}.

G. A. McVean and N. J. Cardin. Approximating the coalescent with recombination. *Philosophical Transactions of the Royal Society B: Biological Sciences*, 360(1459):1387–1393, 2005.

M. Möst, S. Oexle, S. Marková, D. Aidukaite, L. Baumgartner, H.-B. Stich, M. Wessels, D. Martin-Creuzburg, and P. Spaak. Population genetic dynamics of an invasion reconstructed from the sediment egg bank. *Molecular Ecology*, 24(16):4074–4093, Aug. 2015. ISSN 1365-294X. doi: 10.1111/mec.13298.

K. Nara. Spores of ectomycorrhizal fungi: ecological strategies for germination and dormancy. *New Phytologist*, 181(2):245–248, Jan. 2009. ISSN 0028-646X, 1469-8137. doi: 10.1111/j.1469-8137.2008.02691.x. URL https://onlinelibrary.wiley.com/doi/10.1111/j.1469-8137.2008.02691.x.

M. Nei and W. H. Li. Mathematical model for studying genetic variation in terms of restriction endonucleases. *Proceedings of the National Academy of Sciences*, 76(10):5269–5273, Oct. 1979. ISSN 0027-8424, 1091-6490. doi: 10.1073/pnas.76.10.5269. URL https://pnas.org/doi/full/10.1073/pnas.76.10.5269.

L. Nunney and A. E. K. Ritland. The Effective Size of Annual Plant Populations: The Interaction of a Seed Bank with Fluctuating Population Size in Maintaining Genetic Variation. *The American Naturalist*, 160(2):195–204, 2002. ISSN 0003-0147. doi: 10.1086/341017. URL https://www.jstor.org/stable/10.1086/341017.

P. Pavlidis, D. Živković, A. Stamatakis, and N. Alachiotis. SweeD: Likelihood-Based Detection of Selective Sweeps in Thousands of Genomes. *Molecular Biology and Evolution*, 30(9):2224–2234, Sept. 2013. ISSN 0737-4038. doi: 10.1093/molbev/mst112. URL https://www.ncbi.nlm.nih.gov/pmc/articles/PMC3748355/.

T. Sellinger, D. Abu Awad, M. Möst, and A. Tellier. Inference of past demography, dormancy and self-fertilization rates from whole genome sequence data. preprint, Evolutionary Biology, July 2019. URL http://biorxiv.org/lookup/doi/10.1101/701185.

T. P. P. Sellinger, D. Abu-Awad, and A. Tellier. Limits and convergence properties of the sequentially Markovian coalescent. *Molecular Ecology Resources*, 21(7):2231–2248, Oct. 2021. ISSN 1755-0998. doi: 10.1111/1755-0998.13416.

W. R. Shoemaker and J. T. Lennon. Evolution with a seed bank: The population genetic consequences of microbial dormancy. *Evolutionary Applications*, 11(1):60–75, Jan. 2018. ISSN 1752-4571. doi: 10.1111/eva.12557.

W. R. Shoemaker, E. Polezhaeva, K. B. Givens, and J. T. Lennon. Seed banks alter the molecular evolutionary dynamics of Bacillus subtilis. *Genetics*, 221(2), 05 2022. ISSN 1943-2631. doi: 10.1093/genetics/iyac071. URL `https://doi.org/10.1093/genetics/iyac071`. iyac071.

P. R. Staab, S. Zhu, D. Metzler, and G. Lunter. scrm: efficiently simulating long sequences using the approximated coalescent with recombination. *Bioinformatics*, 31(10):1680–1682, May 2015. ISSN 1367-4803. doi: 10.1093/bioinformatics/btu861. URL `https://www.ncbi.nlm.nih.gov/pmc/articles/PMC4426833/`.

W. Stephan. Selective Sweeps. *Genetics*, 211(1):5–13, Jan. 2019. ISSN 0016-6731. doi: 10.1534/genetics.118.301319. URL `https://www.ncbi.nlm.nih.gov/pmc/articles/PMC6325696/`.

F. Tajima. Evolutionary relationship of DNA sequences in finite populations. *Genetics*, 105(2):437–460, Oct. 1983. ISSN 0016-6731. doi: 10.1093/genetics/105.2.437.

F. Tajima. Statistical method for testing the neutral mutation hypothesis by DNA polymorphism. *Genetics*, 123(3):585–595, Nov. 1989. ISSN 0016-6731. doi: 10.1093/genetics/123.3.585.

A. Tellier. Persistent seed banking as eco-evolutionary determinant of plant nucleotide diversity: novel population genetics insights. *New Phytologist*, 221(2):725–730, Jan. 2019. ISSN 0028-646X, 1469-8137. doi: 10.1111/nph.15424. URL `https://onlinelibrary.wiley.com/doi/10.1111/nph.15424`.

A. Tellier and J. K. M. Brown. The influence of perenniality and seed banks on polymorphism in plant-parasite interactions. *The American Naturalist*, 174(6):769–779, Dec. 2009. ISSN 1537-5323. doi: 10.1086/646603.

A. Tellier, S. J. Y. Laurent, H. Lainer, P. Pavlidis, and W. Stephan. Inference of seed bank parameters in two wild tomato species using ecological and genetic data. *Proceedings of the National Academy of Sciences*, 108(41):17052–17057, Oct. 2011. ISSN 0027-8424, 1091-6490. doi: 10.1073/pnas.1111266108. URL `https://pnas.org/doi/full/10.1073/pnas.1111266108`.

A. R. Templeton and D. A. Levin. Evolutionary Consequences of Seed Pools. *The American Naturalist*, 114(2):232–249, Aug. 1979. ISSN 0003-0147. doi: 10.1086/283471. URL `https://www.journals.uchicago.edu/doi/abs/10.1086/283471`.

R. Tournebize, V. Poncet, M. Jakobsson, Y. Vigouroux, and S. Manel. McSwan: A joint site frequency spectrum method to detect and date selective sweeps across multiple population genomes. *Molecular Ecology Resources*, 19(1):283–295, Jan. 2019. ISSN 1755-0998. doi: 10.1111/1755-0998.12957.

804 M. Verin and A. Tellier. Host-parasite coevolution can promote the evolution of seed banking
805 as a bet-hedging strategy. *Evolution*, 72(7):1362–1372, 2018. ISSN 0014-3820. URL `https:`
806 `//www.jstor.org/stable/48575279`.

807 R. Vitalis, S. Glémin, and I. Olivieri. When genes go to sleep: the population genetic consequences
808 of seed dormancy and monocarpic perenniality. *The American Naturalist*, 163(2):295–311, Feb.
809 2004. ISSN 0003-0147. doi: 10.1086/381041.

810 W. M. Waterworth, S. Footitt, C. M. Bray, W. E. Finch-Savage, and C. E. West. DNA damage
811 checkpoint kinase ATM regulates germination and maintains genome stability in seeds. *Proceedings*
812 *of the National Academy of Sciences of the United States of America*, 113(34):9647–9652, Aug.
813 2016. ISSN 0027-8424. doi: 10.1073/pnas.1608829113. URL `https://www.ncbi.nlm.nih.gov/`
814 `pmc/articles/PMC5003248/`.

815 C.-A. Whittle. The influence of environmental factors, the pollen : ovule ratio and seed bank
816 persistence on molecular evolutionary rates in plants. *Journal of Evolutionary Biology*, 19(1):
817 302–308, Jan. 2006. ISSN 1010-061X. doi: 10.1111/j.1420-9101.2005.00977.x.

818 C. G. Willis, C. C. Baskin, J. M. Baskin, J. R. Auld, D. L. Venable, J. Cavender-Bares, K. Donohue,
819 R. Rubio de Casas, and NESCent Germination Working Group. The evolution of seed dormancy:
820 environmental cues, evolutionary hubs, and diversification of the seed plants. *The New Phytologist*,
821 203(1):300–309, July 2014. ISSN 1469-8137. doi: 10.1111/nph.12782.

822 D. Živković and A. Tellier. Germ banks affect the inference of past demographic events. *Molecular*
823 *Ecology*, 21(22):5434–5446, Nov. 2012. ISSN 1365-294X. doi: 10.1111/mec.12039.

824 D. Živković and A. Tellier. All But Sleeping? Consequences of Soil Seed Banks on Neutral and
825 Selective Diversity in Plant Species. In R. J. Morris, editor, *Mathematical Modelling in Plant*
826 *Biology*, pages 195–212. Springer International Publishing, Cham, 2018. ISBN 9783319990705.
827 doi: 10.1007/978-3-319-99070-5_10. URL `https://doi.org/10.1007/978-3-319-99070-5_10`.